

THE PRINCIPAL POINT AND CCD CAMERAS

By T.A. CLARKE¹, J.G. FRYER² and X. WANG¹

1. Department of Electrical, Electronic, and Information Engineering, City University, London, UK.
2. Department of Civil Engineering and Surveying, The University of Newcastle, Australia.

Abstract

The principal point has long been regarded as one of the fundamental parameters in camera calibration. In the age of film based aerial and large format terrestrial cameras' the principal point could be located by a variety of techniques with a certainty of +/- 10 mm (Carman & Brown, 1961) and this was considered sufficient. However, aerial cameras were precision, purpose built, expensive pieces of equipment where the assembly was painstaking and the location of the principal point measured to a known tolerance. In the digital era photogrammetrists, and many others, are using cameras which have not been specifically designed or built for photogrammetry. For these cameras there is no requirement for the manufacturers to position the lens in a pre-defined location relative to the image sensing plane or for the lens manufacturer to align the lens elements precisely. In fact, deviations from the centre of the sensor can be a considerable percentage of the extent of the sensor (up to 10 per cent for some zoom lenses. (Burner, 1995)). This paper discusses the development of methods of obtaining the location of the principal point, considers the relationship between the principal point and other parameters in the functional model, and shows how the location of this point can be estimated with and without recourse to autocollimation methods.

INTRODUCTION

In most text-books on photogrammetry (for example, Atkinson, 1996), the principal point is defined as "that point on the image plane which is at the base of the perpendicular from the 'centre of the lens', or more correctly, from the rear nodal point". In a perfectly assembled camera, the intersection of lines joining the fiducial marks will give a fiducial centre which will coincide with the principal point. The length of that perpendicular is the principal distance and, at infinity focus, it is equal to the focal length of the lens. These definitions are for the situation where the image plane is at right angles to the optical axis of the lens and the lens is a simple one which can easily be thought of as having a readily defined centre. In reality this ideal situation does not exist.

In each era of photogrammetric development it has become necessary to improve methods of calibration and calibration models. Often subtle distortion effects were hidden because the resolution of the system was so poor. For example, prior to the 1950s decentring distortion was not considered a problem and the principal point could be simply defined. Decentring distortion is the non-symmetric departure of rays from co-linearity caused by the misalignment of lens elements during assembly. As the resolution of film improved it became important to take into account the effect of decentring. Hence, a definition of a principal point of best symmetry was used which enabled the decentring effects to be minimised but not modelled or eliminated. Further improvements in the resolution of film and the development of computers and least squares estimation (LSE) methods allowed improved modelling of decentring distortion and the use of a principal point position which was estimated simultaneously with other parameters. At the present time improvements in film based methods have stabilised, but new improvements are constantly being sought in the use of digital images. Such images are acquired from small CCD sensors and cheap lenses. For real-time systems, images are constantly acquired, used, and discarded. Under such conditions it is necessary that LSE processes are optimal and that appropriate parameters are used. If parameters such as those which describe the principal point location are stable over long periods then it may be beneficial only to estimate their value periodically so reducing the number of parameters to be estimated. Further, since real-time systems may be required to continue operation with fewer than the optimum number and distribution of points in 3-D for accurate calibration, this provides a further argument for choosing a good methodology for initial estimation. This paper

reviews the historical development of principal point location methods and attempts to clarify some subtle aspects of principal point parameter estimation. The use of “plumb-lines” and autocollimators as practical means of estimating the location of the principal point for digital cameras are also discussed.

HISTORIC REVIEW OF THE LOCATION AND USE OF THE PRINCIPAL POINT

Aerial camera lenses are composed of several elements and the total assembly will occupy a volume of several hundreds of cubic centimetres. These lenses are assembled in a meticulous fashion. Brown (1966) states that the suppression of decentring distortion to less than five microns over the image format requires considerable skill and that an error of less than two microns would be exceptional. In 1984 (Beamish, 1984) it was stated that great pains were taken in the manufacture and assembly of photogrammetric lenses to achieve perfect centring. It was rare for a lens to have a maximum decentring distortion of under $3\ \mu\text{m}$ and the average was usually between $4\ \mu\text{m}$ and $7\ \mu\text{m}$ for lenses costing £60k. Optical designers state that a tolerance of the magnitude of $\pm 30\ \mu\text{m}$ for the centring of the optical axis with respect to the mechanical axis is a typical tolerance in the manufacture of lenses. For a lens with optical elements of approximately 12 mm diameter, and a 8.5 mm focal length, decentring of around $5\ \mu\text{m}$ would be expected (Smith, 1990). The centre of the lens is not a point which is easy to locate physically and the principal distance has to be determined by optical or photographic means involving some measurements and computations. If a lens had zero radial and tangential distortion, or if all distortions were radial (i.e. perfectly symmetric to the centre of the image format), then the definition and determination of the principal point would not pose any significant difficulty. Unfortunately, this is rarely the case.

The ‘best location’ for the principal point is a topic which has occupied the thoughts of camera calibration authorities and photogrammetrists for much of the twentieth century. Various solutions were suggested, and methods involving banks of collimators, goniometers, autocollimating telescopes and finally self-calibrating LSE procedures found favour at different times. Roelofs (1951) probably produced the most definitive study to that point in time and clearly defined the options for the photogrammetric community. He stated that “pre-war literature contains little of fundamental importance” with relevance to the definition of and methods of obtaining of the principal point - he gives fifty references up to 1939. Roelofs mentioned the method of autocollimation for determining the principal point, but he dismissed it as it required a specialised autocollimating telescope and believed that it was not really the most satisfactory point as it paid no attention to the symmetry, or asymmetry, of the lens distortions. He discussed six different definitions of the principal point. He wished to introduce a new terminology for a ‘calibrated principal point’. He argued along lines similar to those for the calibrated focal length. It was well known that by varying the focal length that the magnitude of the radial lens distortion could be “...distributed over the entire picture plane”. Roelofs suggested that, by examining the radial and asymmetric distortion, a point could be chosen “...to make the distortion symmetrical or asymmetrical to a prescribed amount”. This point would be his calibrated principal point. Its value was for use with stereo-plotting instruments which employed a compensating glass plate or a lens with equivalent distortion to the aerial camera, or mechanical means to vary the focal length. Each of these systems needed a principal point which could be located relative to the distortions present in the image, and he presented a technique to calculate the offsets from the centre of the image plane. Tayman and Ziemann (1984) stated that the principal point of autocollimation is the type of “principal point” which can be determined most directly and accurately. They also defined that the principal point of best symmetry “... is a point near to the principal point of autocollimation chosen so that, when it is used instead of the principal point of autocollimation as a new origin for distortion measurement, it makes the largest absolute difference between new radial measured distortion and new average radial distortion as small as possible along each diagonal of the image format.”

Camera calibration authorities had refined their techniques by 1950 to produce values for the principal point to approximately $\pm 20\ \mu\text{m}$, and had discovered to their dismay that some lenses were exhibiting an asymmetric distortion which was referred to as ‘the prism effect’ of the same magnitude (see for example, Pestrecov, 1951). The prism effect was understood by some photogrammetrists to be a good model for effects caused by slight misalignment of the lens elements and the term ‘decentring

distortion' later became popular after Brown (1966) described its effect and mathematically modelled it. Brown was able to show in 1966 that the prism model was in precise agreement with the tangential component of decentring distortion but at variance by a factor of three with regard to the radial component. However, if translation of the image plane and tipping of the lens with respect to the image plane were taken into account then the model was approximately equivalent. More significant than the correctness or incorrectness of the prism model was the rigour of the derivation of the model and the reasons for its use. There is little justification for the use of the prism model although even today it is still used to explain the effect of decentring (Smith, 1990). However, it should be noted that the widespread acceptance of the prism model as an explanation for decentring distortion was based on the fact that measurements were not conducted to a level that found unmodelled decentring distortion effects to be a problem. In fact although the effect was explained by use of the prism effect, no corrections were actually based on the use of the model, instead the principal point of symmetry was used to spread the asymmetric components of distortion as equally as possible along the image plane diagonals. It was the simultaneous development of self calibration based on LSE procedures that led to a better model. Brown in 1966 stated "accuracies of calibration four to five times greater than those generally considered adequate in conventional mapping are needed if the fullest benefits of analytical methods are to be realised". By using LSE procedures it was possible not only to estimate additional parameters for decentring distortion but also to use them in the estimation of object co-ordinates. The use of such techniques led in turn to the realisation it was not necessary to use a lens which had been specifically manufactured for photogrammetric purposes and that image quality could be considered the paramount feature.

The use of lenses which were not designed for photogrammetric purposes was pioneered by Brown and has continued to this day. It may be argued that Brown's model has been more widely applied (with only minor changes) to cameras and lenses that even he may have considered possible. For instance, lenses which are feasible for use in photogrammetry can be: cheap zoom lenses found in video cameras, typical C mount lenses of some 15 mm in diameter, lenses found in miniature cameras, and "pin-hole" lenses of only 3 mm in diameter. It is pertinent then to consider that the lens designer's main objective in producing any lens is to minimise aberrations. Of the seven aberrations typically considered (spherical, chromatic, lateral chromatic, coma, astigmatism, field curvature, and curvilinear distortion) only one concerns distortion. In books on optical design distortion is often only briefly considered. Its presence may be accepted as a sacrifice to obtain other beneficial effects (Langford, 1982). Lenses typically used in CCD cameras exhibit distortion of fish eye proportions as the focal length is shortened. Photogrammetric considerations are far from the mind of developers of CCD cameras costing less than £100. Therefore it should not be expected that the principal point will be conveniently located at the centre of the image format or that the image plane will be correctly oriented. Hence, if photogrammetric practitioners continue to develop systems using cheap lenses and sensors for an increasingly wide range of applications, especially those involving real-time measurement, the issue of the appropriateness of the models currently used may have to be considered again. Two examples of a trend towards the analysis of unmodelled effects can be seen in the work of Burner (1995), and Fraser *et al.* (1995). Burner discussed the effect of misalignment of the lens with respect to the sensor and concluded that the parameters P_1 and P_2 were able to compensate for misalignments of 0.5 degrees with residual errors as small as a few hundredths of a pixel. He also discussed the use of the point of symmetry (x_s, y_s) as distinct to the principal point (x_p, y_p) . He concludes that "... special measures to properly align the zoom lens to the sensor image plane are probably not necessary, but that as the accuracy obtainable in digital photogrammetry approaches the 0.01 pixel or less level, the use of separate reference point for distortion and photogrammetric computation should be considered". Fraser *et al.* (1995) discussed whether a model for CCD sensor unflatness is necessary for large format sensors which are now being increasingly used. This discussion has similarities with the discovery and subsequent modelling of film unflatness and film shrinkage (Fryer, 1988), and with the increase in CCD sensor size may assume a similar importance in the future.

METHODS OF LOCATING THE PRINCIPAL POINT

Autocollimation methods for aerial cameras

Methods of finding the principal point of autocollimation for film cameras at infinity focus fall into two categories. The first (Fig. 1) is performed with a horizontal camera optical axis and uses two collimators which are in alignment with each other and the replacement of one of the collimators by a mirror surface (Field, 1946).

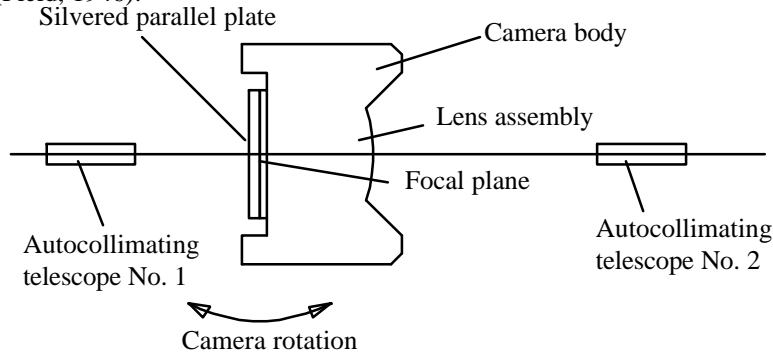


Fig. 1. Dual collimator method of finding the principal point

The second method is performed with a vertical camera optical axis and uses a mirror surface in place of autocollimating telescope No. 2 in Fig. 1 (Fig. 2).

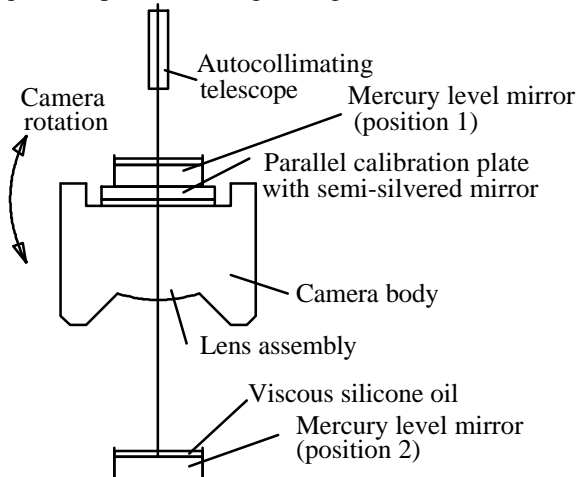


Fig. 2. Single collimator and a level mercury mirror surface.

These methods, or variants on the same scheme, were used for film camera calibration at infinity focus. The next method can be used with CCD cameras at any focal setting.

Autocollimation method for CCD cameras

A method which can easily be used to find the point of autocollimation uses a laser which is mounted in such a way that it can be adjusted to impinge on the centre of the sensor array and be perpendicular to the image plane. With the laser and the camera in such a configuration the laser beam is attenuated and the lens fitted. Provided that the camera and laser are still in the same configuration, then the location of the focussed parallel beam of the laser is at the point of autocollimation. There are two physical disadvantages of this method: first, the camera cannot easily be calibrated in its working position; second, the location of the point of autocollimation is not guaranteed to remain stable if the lens is knocked, adjusted, or removed and replaced. Hence, useful though this method is, in that it is independent of LSE procedures and avoids correlation with other parameters, it is ultimately not a practical method. When adjusting the sensor surface to the desired orientation with respect to the laser

beam, the reflected beam must be arranged to return along the same path as the incident beam. Care must also be taken not to confuse the returned reflection from any protective cover glass mounted in front of the sensor. The laser beam is coherent and monochromatic and the observed reflections are a diffraction pattern caused by the micro-structure of the silicon surface of the sensor. This diffraction pattern is both regular and symmetric. If the laser is projected through a small hole as shown in Fig. 3, the returned beam must be aligned to return through this hole. The intensity of the diffraction peaks diminishes from the central peak, which is surprisingly similar to its nearest neighbours, and alignment can be achieved not only by using the central peak but also using the maxima either side of the main peak.

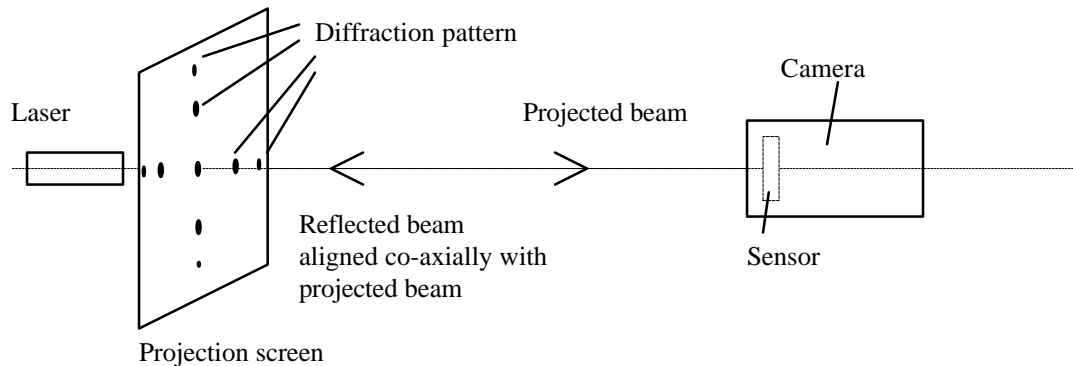


Fig. 3. Configuration of the laser and sensor.

Attenuation of the laser can be achieved by using parallel sided neutral density filters, or by use of the exposure control for the CCD camera. In this way the point of autocollimation can be found by locating the image of the laser beam with a typical aperture setting. It should be noted that speckle effects caused by the laser beam will cause the image of the laser beam to be falsely located (Clarke and Katsimbrus, 1994). For this reason it is reasonable to assume accuracy only to the nearest pixel for the point of autocollimation. It is also worth checking that all algorithms use the same image size and investigating the operation of the frame-grabber as the full sensor size is not always digitised.

Determination of the principal point location by analytical techniques

Once the work of Brown (1971) had been widely understood by the photogrammetric community, the use of self-calibrating LSE procedures as a means to calibrate cameras became widespread. Access to computers had become easier and programming in languages, such as FORTRAN, was being taught in undergraduate classes. The basis for the self-calibration method is now well known and can be found in photogrammetric textbooks, for example Wolf (1983). The collinearity equations are extended by the inclusion of terms for the parameters of inner orientation and lens distortion and, using LSE procedures, estimates of these parameters and of the 3-D co-ordinates of the object targets and the exterior orientation parameters of the cameras are produced. For a satisfactory solution, the geometry of the entire network must be strong. This means a wide range of camera orientations, usually 4 or more camera locations and a 3-D set of at least 50 targets which are visible from all camera locations. Since all parameters are solved for simultaneously, consideration of the correlations which exist between the elements of interior and exterior orientation, for example, must be understood by the photogrammetrist. If terms such as x_p and y_p are to be determined, and it is thought that these will be invariant from image to image, an understanding of which other parameters are strongly correlated with them will aid the design of a suitable network.

The LSE process applied to a non-linear set of equations, such as collinearity equations, involves iterations on the first order derivatives of the parameters. Therefore trial values are entered for all the unknown parameters (even if the trial value is zero). To “constrain” this process so that it will converge to a global minimum, it may be necessary to assign expected standard errors to the parameters. It is at this point that the authors wish to note the difference between self calibrating LSE procedures for CCD cameras and conventional film based ones. The implicit assumption that the centre of the optical

axis will be very close to the centre of the imaging format is not necessarily valid for CCD cameras. In fact the values of x_p and y_p may be so large as to render invalid the first order approximations to the basic collinearity equations. A single solution to the self calibrating LSE process may not produce results which will meet the stringent demands of later use in real-time industrial photogrammetry. Some researchers, for instance Shortis *et al.* (1995), found it necessary to iterate the entire process more than once to ensure that the trial values for the image co-ordinates, which affect the results for the parameters of radial and decentring distortion, are re-calculated based on successive estimates for x_p and y_p .

THE CONNECTION BETWEEN THE PRINCIPAL POINT AND LENS AND ORIENTATION PARAMETERS

Introduction

The functional model generally used in photogrammetric LSE procedures uses the principal point location as a parameter in a typical LSE using minimum constraints. Correlations are known to exist between parameters in such cases. If the network is geometrically weak, such correlations may lead to instabilities in the LSE process. The combination of the network configuration and physical camera characteristics will be modelled using most, but possibly not all, of the available parameters. If real-time systems are considered it will be sensible if certain parameters, such as the principal point parameters, are measured and used in any subsequent LSE constrained by their standard deviation, or even fixed. This is because it would be expected that such parameters will not change significantly over long periods of time. Under these circumstances it is essential to understand the effects of such a constraint.

To gain an understanding of the relationship between the principal point and other parameters, the commonly used functional model can be examined under various conditions. The main assumption is that the functional model correctly models real effects. If this were not largely so, the residuals from measurement processes would not be as low as they typically are, so this assumption is likely to be reasonably valid. Hence, given that these effects exist, and no other significant systematic errors or unmodelled effects are present, it may also be assumed that a global minima will exist in which these parameters will adjust to optimum values to minimise the error of the target function. However, if any of these parameters are fixed at any other values, the global minimum will not be attained. It is likely that the result may not be grossly different from the best estimate, as under these conditions any parameters which have similarities to the fixed parameter may adjust to what are incorrect values to compensate. Parameters which have no similarities would be unlikely to be affected significantly. Hence, to understand the effect of an error in the location of the principal point it is possible to compare the modelling achieved by other parameters which have similar characteristics. This process is complex, but by analysing the correlations one at a time it is possible to gain a clear understanding of what happens in LSE processes. The main parameters which have characteristics with similarities to the principal point location are: decentring distortion parameters P_1 and P_2 , and the exterior orientation parameters ω and ϕ . These relationships are now analysed.

Correlation between parameters

Correlation coefficients are obtained directly from the covariance matrix which results from a LSE procedure using a given set of observation equations and a functional model. The magnitude of the correlation coefficient describes the interrelationship between parameters. High correlation coefficients imply high correlations between the relevant parameters. However, the correlations obtained are dependent on the parameters being adjusted, the observation equations, and the network configuration. Data on target image location were obtained from 66 targets placed on a 3-D test field and imaged by a single camera positioned in four locations with a convergent angle of approximately 90 degrees. LSE with minimum constraints was performed and the full co-variance matrix produced. The parameters which showed a high level of correlation are shown in Table I.

TABLE I. Correlation coefficients for some of the adjusted parameters.

<i>Parameter 1</i>	<i>Parameter 2</i>	<i>Correlation coefficient (%)</i>
ω	x_p	98.47
ω	P_1	93.78
ϕ	y_p	96.95
ϕ	P_2	78.14
x_p	P_1	93.51
y_p	P_2	76.39
K_1	K_2	97.60
K_2	K_3	98.62
K_3	K_1	92.96
c	Z	94.45

K_1 , K_2 , and K_3 are radial lens distortion parameters and c is the focal length. This table illustrates that in this case the external orientation angles (ω and ϕ) are linked to the principal point (x_p , y_p) and to the decentring distortion parameters (P_1 & P_2), and that the principal point is linked with the decentring distortion parameters. These relationships are well known. Furthermore, the principal distance is related to the Z co-ordinate of the camera position (under the condition of inner constraints). If the external parameters ω and ϕ are held fixed in the LSE then a new set of correlations can be analysed between the interior parameters only. The results are illustrated in Table II.

TABLE II. Correlation between parameters with fixed external orientation.

<i>Parameter 1</i>	<i>Parameter 2</i>	<i>Correlation coefficient (%)</i>
x_p	P_1	76.63
y_p	P_2	77.42
c	K_1	94.37
c	K_2	86.09
c	K_3	78.34
K_1	K_2	97.59
K_2	K_3	98.54
K_3	K_1	92.80

These correlation coefficients show that the correlations between the radial distortion parameters (K_1 , K_2 , and K_3) were unaffected by the exterior orientation parameters, but that the correlations between the principal point and the decentring distortion were considerably lower implying that much of the correlation is caused by the exterior orientation parameters. Finally, the principal distance c is now strongly correlated with the radial distortion parameters. However, it can be noted from these observations that the correlation coefficients alone do not indicate all of the relationships which are possible between parameters. The functional relationships between parameters are now investigated by individually comparing models to find the extent to which the correlation parameters indicate the potential of one parameter to be replaced by another.

Example of modelling similarities

As an example, the relationships between the radial lens distortion parameters K_1 , K_2 , and K_3 (which often have high correlation coefficients) are discussed. The influence of these parameters is conceptually easy to grasp, being odd order polynomials of order three, five, and seven respectively. Lens distortion is mapped relative to the principal point and is a function of the radial distance. These functions can be plotted and the similarities in their shape analysed. To do this a realistic value for K_1 was chosen and graphs using K_2 , K_3 , and K_2 and K_3 were plotted, where the values of K_2 and K_3 were chosen to minimise the difference between the K_1 curve and that generated with the other selected parameter(s). Fig. 4 & 5 illustrate the difference between the curves generated by the parameters.

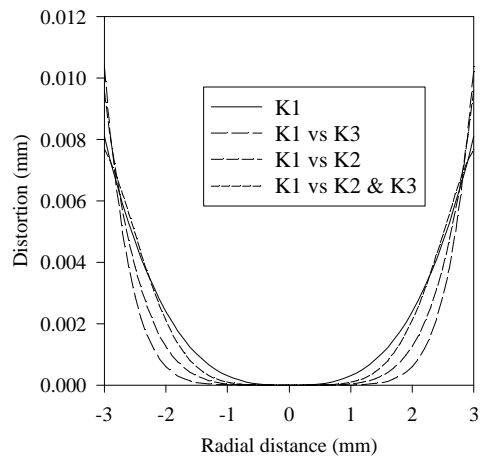


Fig. 4. Comparison between curves generated using K_1 , K_2 , and K_3 (absolute values).

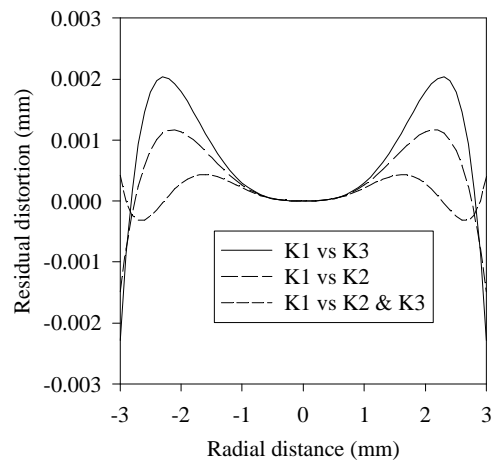


Fig. 5. Comparison between curves generated using K_1 , K_2 , and K_3 (differences).

The graphs illustrate that the K_2 and K_3 can separately, or together, produce a distortion map which is similar to that obtained using K_1 alone. However, errors must be introduced if the underlying distortion is best described with K_1 alone. Hence, even exceptionally high correlation coefficients do not imply that one parameter can be dropped without consequence.

Decentering and the location of the principal point

Any discussion of the principal point must also consider decentering distortion as both appear to be linked except, of course, for the case of a perfect lens. Fraser *et al.* 1995 state “There is a strong projective coupling between the decentering distortion parameters (P_1 , P_2) and the principal point offsets (x_p , y_p). This correlation has practical consequences in self calibration for it means that to a significant extent decentering distortion effects can be compensated for by a shift in the principal point (and an effective shifting of the optical axis).” Statements of this kind have often been made and superficially appear correct, but, it is the postulate that decentering effects can be compensated for “to a significant extent” that is considered here. Slama, 1980 offered the opinion that “.... decentering coefficients also interact to a moderate degree with x_p and y_p .” Burner, 1995 concluded that the parameters P_1 and P_2

were able to compensate for physical misalignments of the lens of 0.5 degrees (with respect to the optical axis) to several hundredths of a pixel.

It is instructive to assess how accurately the model for decentring actually compensates for a shift in the principal point. For instance, could the principal point be fixed at an arbitrary value and the decentring distortion be used to compensate for the incorrect value of the principal point? If so, to what extent would this be possible - 10 pixels, one pixel? This is a superficially appealing idea because it would imply that an accurate estimation of the principal point is unnecessary. Some justification for such a postulate could be taken from the observation of correlation coefficients between P_1 and x_p of 98 per cent. However, it will be shown that such an idea is flawed.

A vector plot of the differences between the functional model for a displacement of $x_p = 10 \mu\text{m}$ and the functional model for P_1 were computed at discrete positions. The simulated image plane was 800×600 pixels in size. A value of P_1 was chosen to minimise the r.m.s. of the differences computed at regular grid positions throughout the simulated image (only P_1 was used as the shift was only in the x direction). A graph of the differences is illustrated in Fig. 6.

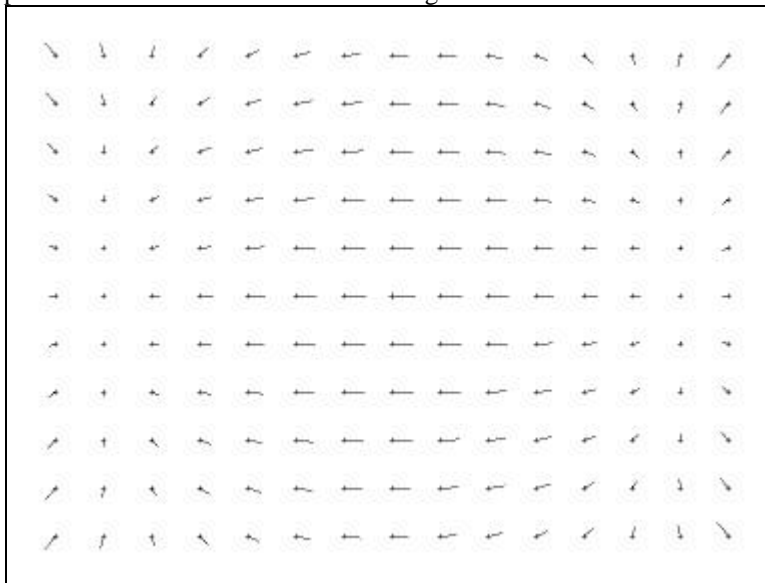


Fig. 6. Vector differences between models for principal point shift when P_1 is used to compensate. The scale of each vector is 0.4 times the grid spacing.

Similar graphs could be produced for other combinations of x_p and y_p , with compensating values for P_1 and P_2 . The resulting r.m.s. error was $6.57 \mu\text{m}$. It is clear that to only a surprisingly small extent (the r.m.s. error was reduced by 34 per cent) P_1 and P_2 can compensate for x_p and y_p shifts. This was not expected from the correlation coefficients and the quotations cited earlier. To explain this apparent discrepancy, further consideration of parameters which may be expected to compensate for principal point shifts are now discussed.

Exterior orientation and principal point.

It was noted previously that there was a strong correlation between the exterior orientation parameters and the principal point. To investigate this, the same principal point shift was modelled as in the previous section and the exterior orientation of the camera used to compensate. Again a value for the orientation was found that minimised the discrepancies between the models. The differences were then mapped as displacement vectors (Fig. 7).

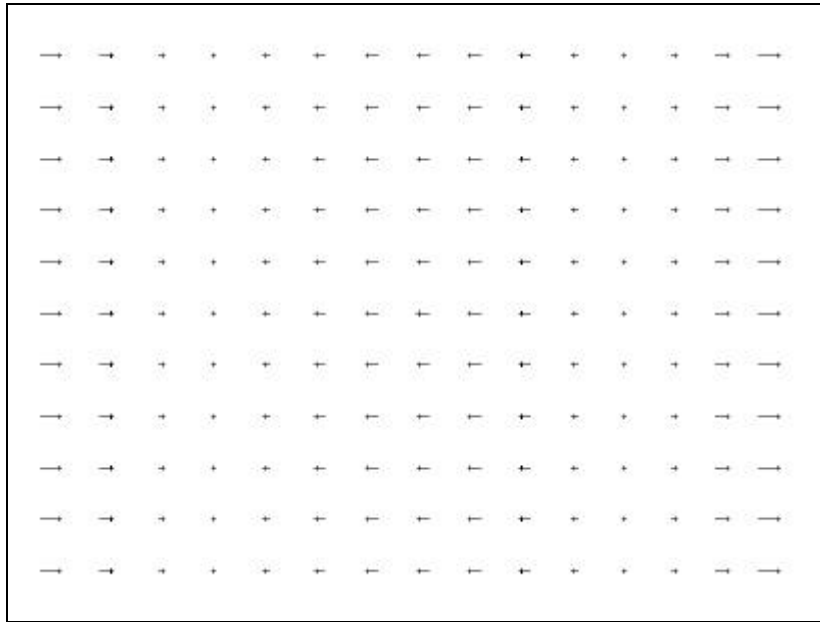


Fig. 7. Displacement vectors showing discrepancy between the effect of camera exterior orientation and x_p modelling. The scale of each vector is four times the grid spacing.

The r.m.s. of the differences was reduced by 96 per cent to $0.43 \mu\text{m}$. Fig. 7 illustrates that these models are similar to each other, clearly explaining the correlations between these parameters in this particular case.

Exterior orientation, principal point shift, and decentring distortion..

The residual distortion shown in Fig. 7 has some similarities with decentring distortion. To investigate this, decentring distortion using P_1 was introduced to see whether this parameter could reduce the residuals on the image plane. It was found that the residual distortion could be reduced from 0.46 to $0.34 \mu\text{m}$. Further reductions were also found to be possible by adjusting P_1 and the exterior orientation parameters together so that a residual distortion of $0.24 \mu\text{m}$ was achieved (a reduction of 98 per cent). The remaining distortion appeared to have no similarity with any other part of the functional model so no further reductions were considered likely. At this point it is possible to explain the statements made by Burner (1995), Slama (1980), and Fraser *et al.* (1995). The potential usefulness of P_1 and P_2 (which is implied in the level of their correlations with x_p and y_p) is as a result of a discrepancy in the modelling between exterior orientation and the principal point shift. This discrepancy can be reduced by use of P_1 and P_2 to a significant extent (the r.m.s. image residual was approximately halved). To be fair to the authors quoted, it is likely that they implicitly understood that the exterior orientation was the link causing the correlation between the parameters, but, it is hoped that this investigation has resolved any ambiguity.

The relationship of radial and decentring distortion to the principal point.

A final point that should be made in this section is that radial lens distortion will often be defined with respect to the principal point. This raises the worrying possibility of another error source which is the mismatch in distortion modelling tied to an erroneous principal point location. To consider this aspect two radial lens distortion curves were produced with a difference in principal point location of $10 \mu\text{m}$, as in the previous cases, and also of $200 \mu\text{m}$ (Fig. 8).

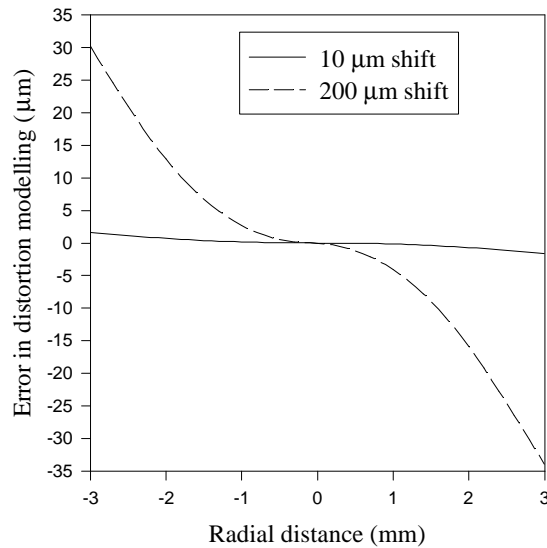


Fig. 8. Radial lens distortion differences between curves with no displacement and displacements of 10 μm and 200 μm respectively.

The error in mapping caused by shifts in co-ordinates, which are not compensated by a principal point displacement, is relatively small for a 10 μm shift being a maximum of 1.6 μm at a radial distance of 3 mm, but reached 33 μm at a radial distance of 3 mm for a 200 μm shift.

Conclusion

The previous discussions have been able to clearly expose the fundamental relationships between parameters. It is important to reiterate that no attempt has been made to imply that these relationships actually represent real distortions or effects. The method of analysis was merely a device to clarify issues. The practical reality may be something which is not perfectly modelled by any combination of radial and decentring lens distortion parameters.

ESTIMATING THE PRINCIPAL POINT OF CCD CAMERAS

Having considered the importance of knowing the location of the principal point and various methods for its location, this section considers the use of the plumb line method, together with a LSE procedure, as a means of estimating the location of the principal point. The reasoning behind this method is that, given that the plumb line method can provide good estimates of radial and decentring distortions, it is possible to estimate the remaining unknown parameters, for instance x_p and y_p , with a simultaneous LSE with the known parameters fixed or constrained by their standard deviations. If the solutions for radial and decentring distortion are accurate, then the solution for the remaining parameters will be stronger and independent of correlations that may otherwise affect the results of a LSE process with minimum constraints using all of these parameters. It will be shown that while the radial lens distortion parameters can be estimated reasonably well with poor estimates of the principal point location, the decentring distortion parameters are sensitive to such an error.

The use of straight lines to perform calibration of lenses was first presented to the photogrammetric community by Brown (1971). His first application of the technique was described in a technical report in 1962 and this original description of the method “involves photographing a set of plumb lines arrayed in the desired object plane and exploits the fact that, in the absence of distortion, the central projection of a straight line is itself a straight line. Systematic deviations of the image of the

plumb lines from straight lines thus provided a measure of distortion if properly reduced". The use of this method is well known (Fryer and Brown, 1986) and so is not described further except to note some observations of Brown concerning the recovery of the principal point. Brown's original derivation of the plumb line LSE carried x_p and y_p as adjustable parameters. However he found that these parameters were inherently indeterminate if P_1 and P_2 were also estimated. In fact, even if P_1 and P_2 were not estimated, the recovery of x_p and y_p was found to be very weak and accurate to only 200 μm (one sigma) .

Simulation with varying principal point offset

A pertinent question to ask at this point is whether the lens distortion parameters can reliably be estimated given that the principal point location is unknown and that the best guess for its location (centre of image format for instance) may be significantly wrong. Such a situation is often encountered due to differences in hardware, software, or camera manufacture. For instance, the nominal centre of the image may be computed by dividing the maximum x and y dimensions by two. Frame-grabbers use various methods for counting the number of pixels from a nominated beginning to the end of an image. It is not unusual for a black area of four pixels to be encountered due to the image digitisation occurring too early in the video line. This may mean that four pixels are effectively missing from the edge of the image. An Epix frame grabber (Epix, 1991) allows the image horizontal size to be selected only in multiples of four pixels. A difference in image co-ordinate centre of over ten pixels was recently encountered purely due to the size of image used in two different software programs. In addition to this type of variation in image co-ordinates, the location of the principal point can vary considerably from camera to camera due to the fact that for many cameras the position of the sensor with respect to the lens is not considered important as it makes little difference to the visual quality of the image. This situation must be contrasted with the type of lens used for early photogrammetric purposes where differences between the fiducial centre and the principal point of best symmetry or autocollimation were very small compared with the size of the image format.

To investigate the effect of large errors in the nominal centre of an image in a CCD camera, a number of simulated plumb line sets were created with realistic values used for the parameters of radial and decentring distortions. These values were of the same size and magnitude as those found in practical tests with typical cameras. The parameters of radial and decentring distortions were kept constant and the offsets of the principal point from the centre of the simulated sensor array were varied in steps of 20 μm from 0 - 200 μm in two directions at 45 degrees to each other. From these data sets the parameters were estimated by a LSE procedure using the method described by Brown (1971). Having obtained a reasonable solution for each set, comparisons were then made by differencing the two sets at discrete positions in the image (Fig. 9).

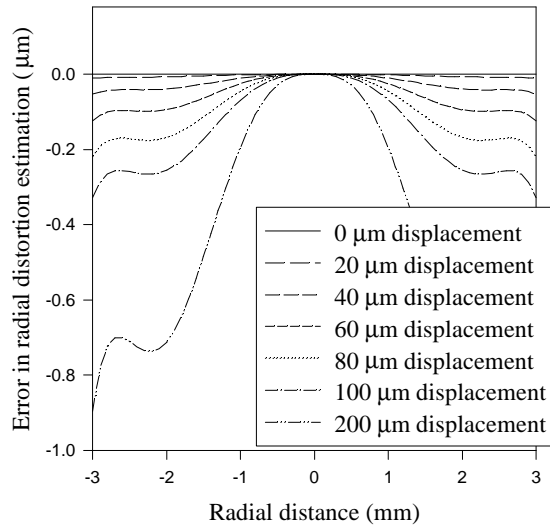


Fig. 9. Radial distortion error introduced with various image offsets.

With no error in the location of origin of the simulated image co-ordinates, the parameters were estimated with no significant difference between the calculated and original values. The small difference just being due to the convergence criteria stopping the LSE process before further improvements were made. As the error in the origin increased so errors were introduced to the parameters which are illustrated in Fig. 9. It is worth noting that with an offset as large as 200 μm (more than twenty pixels), the error introduced at the edge of the format would only be of the order of one tenth of a pixel. Hence, it may be concluded that the plumb line method for estimation of radial distortion, as implemented in the LSE process used, is relatively insensitive to errors in the image centre location.

The effect on the estimation of decentring distortion of varying the origin of the image co-ordinates is now analysed. The decentring parameters from the plumb line calibration were used to compute the difference between the model generated by the parameters with varying degrees of offset. The 45 degree set was used and the distortion was plotted along the 45 degree axis (Fig. 10).

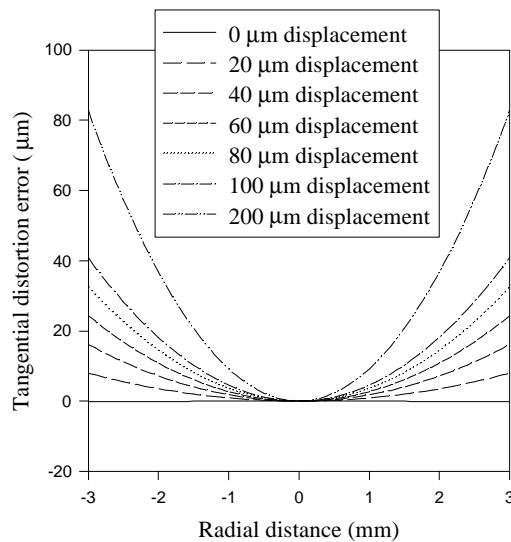


Fig. 10. Decentring errors along the 45 degree axis.

These results show that, unlike radial distortion, decentring distortion estimation using the plumb line method is highly sensitive to image co-ordinate offsets to the extent that the errors are considerably bigger than those encountered in the radial distortion estimation. The explanation for this can be found by considering the effects when the offsets are only in the x direction. Under these conditions the results illustrated in Table III were obtained.

TABLE III. Decentring parameters for x offset only.

	<i>Zero x shift.</i>	<i>200 mm shift in the x direction</i>
P_1	5.0294e-4	-6.8980e-4
P_2	5.0302e-4	5.0390e-4

Table III illustrates that the estimation of the P_2 parameter is virtually unaffected by the shift in the x direction. This should be expected given that the P_2 parameter is related to shifts in the y direction. The magnitude of the P_1 parameter was also similar when the principal point shift was at 45 degrees to the x axis. Hence, it may be concluded that the reason for the very large variations in the P_1 parameter is due to the usefulness of this parameter in the LSE process, this is certainly possible but not without the introduction of significant errors.

ANALYSIS OF RESULTS

The discussions so far have enabled a clear understanding of the relationships between parameters so that it is now possible to analyse how such effects can affect the results of LSE procedures. Lens distortion is defined relative to the principal point. There will be an optimum location of this point as a result of correctly modelling the distortion. It will not be possible to correct for this error by using the decentring distortion parameters to compensate although changes will occur in their values which will be of minor value. Furthermore, it will not be possible to correct for this error using the exterior orientation parameters as these too, although mapping the change in principal point location reasonably well, will not prevent an increase in the lens distortion error from both decentring and radial components.

LSE with free external orientation parameters for each camera, all interior parameters fixed.

To test the conclusions reached concerning the importance of the principal point location, a simulation was performed using a well distributed set of targets and a highly convergent network. After the LSE process, the image residuals were noted along with all other parameters. Displacements as shown in Table IV were introduced to the image co-ordinates and adjustments were performed. The network consisted of four cameras with 100 targets randomly distributed in a rectangular envelope which would be visible from all camera view points. The K_1 , K_2 & K_3 parameters used were 3.38e-3, -2.5e-4, 2.427e-5 respectively. The decentring parameters were 5.0e-4.

TABLE IV. Results of LSE with exterior orientation free.

<i>x image shift (mm)</i>	<i>y image shift (mm)</i>	<i>R.m.s. image residual (mm) (no noise added)</i>	<i>R.m.s. image residual (mm) (2 mm random noise added)</i>
0	0	0	1.98e-4
0.01	0	4.53e-5	2.03e-4
0	0.01	5.05e-5	2.05e-4
0.01	0.01	6.99e-5	2.10e-4
0.05	0.05	3.49e-4	4.00e-4
0.1	0.1	6.96e-4	7.20e-4
0.15	0.15	1.04e-3	1.05e-3
0.2	0.2	1.38e-3	1.39e-3

The results illustrated in Table IV show clearly that the external orientation parameters are able to compensate significantly for shifts in the image co-ordinates; but that this cannot be achieved without error which with a shift of 200 μm was as high as 1.38 μm r.m.s. The source of this error can be

attributed directly to the difference between the functions for exterior orientation and the principal point shift.

LSE with free external orientation parameters for each camera and P_1 and P_2 .

In this case the parameters P_1 and P_2 were also estimated, but x_p and y_p were fixed. The results are given in Table V.

TABLE V. Results of LSE with exterior orientation and P_1 and P_2 free.

x image shift (mm)	y image shift (mm)	P_1	P_2	R.m.s. image residuals (mm)	R.m.s. image residuals (mm) (2 mm random noise added)
0	0	5.00 e-4	5.00e-4	0	1.98e-4
0.01	0	5.2e-4	5.00e-5	3.33e-5	2.01e-4
0	0.01	5.02e-4	5.22e-4	3.28e-5	2.01e-4
0.01	0.01	5.21e-4	5.22e-4	4.7e-5	2.04e-4
0.05	0.05	5.99e-4	6.08e-4	2.39e-4	3.11e-4
0.1	0.1	6.88e-4	7.12e-4	4.9e-4	5.29e-4
0.15	0.15	7.65e-4	8.01e-4	7.54e-4	7.78e-4
0.2	0.2	8.29e-4	9.01e-4	1.03e-3	1.05e-3

These results indicate very clearly that P_1 and P_2 have relatively small roles to play in minimising the r.m.s. errors compared to what is possible with the exterior orientation parameters alone. This confirms the previous result where a reduction in error residuals of about a third was found. It should be noted here that there are some differences between the two methods so it is not possible to make exact comparisons between the r.m.s. residuals in each case. In the initial experiments the observations were evenly distributed over the whole image plane, while in this latter case the observations were randomly distributed; the 3-D objects targets were guaranteed to be imaged by every camera so the observations would not have extended to the edge of the image format in this case; and in the LSE case one camera was used four times which would have resulted in lower image residuals.

LSE with minimum constraints

Finally all of the parameters were freed in a self calibrating LSE procedure and the results obtained under various conditions are illustrated in Table VI.

TABLE VI. Simulation test results from a LSE process with minimum constraints.

Parameter	Values used in image co- ordinate generation	Recovered values after LSE	Recovered values after LSE with r.m.s. image noise = 0.2 mm	Recovered values after LSE with r.m.s. image noise = 0.2 mm and a 20 mm shift in x, y image co- ordinates
x_p (mm)	0.02	2.0000e-2	2.2063e-2	4.2066e-2
y_p (mm)	0.02	2.0000e-2	1.9670e-2	3.9673e-2
δc ($c = 8.5$ mm)	0	-1.1983e-7	7.0106e-4	6.9863e-4
K_1	3.38e-3	3.3800e-3	3.3685e-3	3.3689e-3
K_2	-2.50e-4	-2.5048e-4	-2.4115e-4	-2.4137e-4
K_3	2.42e-5	2.4269e-5	2.3310e-5	2.3344e-5
P_1	5.0e-4	5.0000e-4	4.9544e-4	4.9543e-4
P_2	5.0e-4	5.0000e-4	5.0065e-4	5.0065e-4
R.m.s. image error		0.0	1.98627613e-4	1.98627618e-4

The simulation tests illustrated that, with no image errors, all of the parameters could be recovered to a high level of precision such that the r.m.s. image errors were effectively zero. When random image errors were introduced of 0.2 μm the parameters were not estimated quite so well. However, when the co-ordinates of the images were shifted by 20 μm these shifts were recovered by the LSE process with marginal difference between the two sets and almost no difference in the r.m.s. errors on the image plane. The conclusion is that the modelling of the principal point shift introduces almost no errors if its location can be correctly recovered.

CONCLUSIONS

This paper has discussed the location of the principal point. The history of the development of camera calibration methods with regard to the principal point estimation has briefly been covered. Methods of locating the position of the principal point have been discussed. Correlated parameters have been compared using their functional models. This has proved to be an instructive method of analysing relationships and the degree to which one parameter can adjust to minimise the errors caused when another parameter is constrained to an erroneous value. The way in which P_1 and P_2 are related to x_p and y_p has been clearly explained. Finally, practical tests were conducted which showed that radial lens distortion parameters could be estimated relatively accurately even when significant offsets of the image co-ordinates were present, but that the decentring distortion parameters were sensitive to this error.

From this work it is useful to be reminded that given: a functional model which represents physical effects; target image co-ordinates which are subject to random error; a reasonably large number of 3-D targets which are well distributed; and a highly convergent network, all of the usual parameters can be estimated to reasonable values. However, if there is a deficiency in any one of these areas it can lead to inadequate estimates and to errors. Under these circumstances, which may be common for real-time systems with little control over the measuring environment, alternative strategies will be needed to make full use of the potential of a given system. Furthermore, attention must be paid to even small details, such as the location of the principal point, if residuals are to be optimally minimised.

ACKNOWLEDGEMENTS

The authors wish to acknowledge the contribution of Professors M.A.R. Cooper and M.R. Shortis to various discussions during the preparation of this paper, and Mr. K.B. Atkinson and Mr. D.A. Tait for the provision of some of the references.

REFERENCES

- Atkinson, K.B. (Editor), 1996. *Close range photogrammetry and machine vision*. Whittles Publishing, Caithness, Scotland. 371 pages.
- Beamish, J.K. (Editor), 1984. *Close-range photogrammetry and surveying : state-of-the-art*. Section 1. Tutorials. 1984 ASP-ACSM Fall Convention, San Antonio. American Society of Photogrammetry, Falls Church, Virginia, USA. 941 pages.
- Brown, D.C., 1966. Decentering distortion of lenses. *Photogrammetric Engineering*, 32(3):444-462.
- Brown, D.C., 1971. Close-range camera calibration. *Photogrammetric Engineering*, 37(8):855-866.
- Burner, A.W., 1995. Zoom lens calibration for wind tunnel measurements. *SPIE Vol. 2598*: 19-33.
- Carman, P.D. and Brown, H., 1961. Camera calibration in Canada. *Canadian Surveyor*, 15(8): 425-439.
- Clarke, T.A. and Katsimbris, A., 1994. The use of diode laser collimators for targeting 3-D objects. *International Archives of Photogrammetry and Remote Sensing*, 30 (5): 47-54.
- Epix, 1991. Silicon Video MUX. *User's manual*, version 2.4. 27 pages.
- Field, R.H., 1946. The calibration of air cameras in Canada. *Photogrammetric Engineering*, 12(2): 142-146.
- Fraser, C.S., Shortis, M.R. and Ganci, G., 1995. Multi-sensor system self calibration. *SPIE Vol 2598*:2-18.

- Fryer, J.G. and Brown, D.C., 1986. Lens distortion for close-range photogrammetry. *Photogrammetric Engineering and Remote Sensing*, 52(2):51-58.
- Fryer, J.G., 1988. Lens distortion and film flattening: their effect on small format photogrammetry. *International Archives of Photogrammetry and Remote Sensing*, 27(5): 194-202.
- Langford, M.J., 1982. *Advanced photography*. 4th Edition. Focal Press, London. 397 pages.
- Pestrecov, K., 1951. Calibration of lenses and cameras. *Photogrammetric Engineering*, 17(3): pp. 398-400.
- Roelofs, R., 1951. Distortion, principal point, point of symmetry and calibrated principal point. *Photogrammetria*, 7(2): 49-66.
- Shortis, M.R. Snow, W.L and Goad, W.K., 1995. Comparative geometric tests of industrial and scientific CCD cameras using plumb line and test range calibrations. *International Archives of Photogrammetry and Remote Sensing*, 30(5W1): 53-59.
- Slama, C.C. (Editor), 1980. *Manual of photogrammetry*. 4th Edition. American Society of Photogrammetry, Falls Church, Virginia. 1056 pages.
- Smith, W.J., 1990. *Modern optical engineering - the design of optical systems*. McGraw-Hill, New York, USA. 525 pages.
- Tayman, W.P. and Ziemann, H., 1984. Photogrammetric camera calibration. *Photogrammetria*, 39(2): 31-53.
- Wolf, P.R., 1983. *Elements of photogrammetry*. 2nd Edition. McGraw-Hill, New York, USA. 628 pages.

PAPER REFERENCE

Clarke, T.A. Fryer, J.F. Wang, X. 1998. The principal point and CCD cameras. Photogrammetric Record. Photogrammetric Record 16(92): pp 293-312.